

Article

Numerical Simulation of the Picking Process of Supernormal Jujube Branches

Ren Zhang ¹, Guofeng Wang ^{1,2}, Wei Wang ^{1,*}, Dezhi Ren ¹ , Yuanjuan Gong ¹, Xiang Yue ¹ , Junming Hou ¹ and Mengmeng Yang ¹

¹ College of Engineering, Shenyang Agricultural University, 120 Dongling Road, Shenhe District, Shenyang 110161, China

² Key Laboratory of Liaoning Province for Clean Combustion Power Generation and Heat-Supply Technology, Shenyang Institute of Engineering, Shenyang 110136, China

* Correspondence: syww@syau.edu.cn; Tel.: +86-13-898-179-216

Abstract: This paper elaborates on a digital simulation study on supernormal particle flow used to investigate and analyze the process of picking up jujube branches, which was a meaningful attempt to search for accurate and effective advanced numerical analogy methods in the agricultural field. In this paper, the meshless technology based on the element-free Galerkin method was used for the first time to present the effects of particle size, particle number and particle acting force on the movement of irregular particles, and the influence of the gear rotation speed, the feeding amount, and the jujube branch size on the movement behavior as well as the picking rate. It can describe not only the particles' dynamic movement in the process of picking up jujube twigs, such as feeding, collision, throwing and rolling, but also the effect of the quality and shape caused by the particle size, which in turn affects the surface force of particles and interparticle acting force, thereby affecting the weight function in the analytical solution, the total feeding amount and the effect of the acting force resulting from the particles' contact, roll and collision caused by gear rotation. The findings reveal that the digital simulation, based on the meshless Galerkin technology and Rocky software, is effective in dealing with issues related to supernormal particle flow. By eliminating the influence of geometric shapes on calculations, the method boasts an effective solution to the movement problems of irregularly shaped particles, which would be further applied in the agriculture field.

Keywords: meshless Galerkin method; supernormal particles; jujube branches; picking mechanism; numerical model



Citation: Zhang, R.; Wang, G.; Wang, W.; Ren, D.; Gong, Y.; Yue, X.; Hou, J.; Yang, M. Numerical Simulation of the Picking Process of Supernormal Jujube Branches. *Agriculture* **2023**, *13*, 408. <https://doi.org/10.3390/agriculture13020408>

Academic Editor: Massimo Cecchini

Received: 20 December 2022

Revised: 24 January 2023

Accepted: 25 January 2023

Published: 9 February 2023



Copyright: © 2023 by the authors. Licensee MDPI, Basel, Switzerland. This article is an open access article distributed under the terms and conditions of the Creative Commons Attribution (CC BY) license (<https://creativecommons.org/licenses/by/4.0/>).

1. Introduction

Supernormal particles, particles with irregular geometric shapes whose length is at least several times the diameter, cannot be simplified into a spherical-shape mathematical model. The flow of supernormal particles has the characteristics of anisotropy and involves complex forces, so conventional methods for non-spherical particles such as equivalent diameter, shape factor and specific surface area are not suitable for supernormal particle problems to be solved in the agricultural field [1–3]. Taking the problem of jujube branch picking as an example, since jujube pruning stubs have typical characteristics such as jujube thorns, crotches, sizeable stem-to-length ratio, and high degree of irregularity, the jujube branch picking process is commonly seen as a specific abnormal particle flow problem. Exploring advanced and accurate simulation methods is the key to solving the complex flow problem of agricultural supernormal particles [4–7].

Presently, research on spherical particles, non-spherical particles and slender particles is extensive in the agricultural field, with different algorithms of particle movement being widely applied in various types of research. A two-stage dust removal device for straw carbonization flue gas has been designed by Xin et al. [8] and simulated the separation efficiency of dust particles using the DPM model to test the relationship between the particle

size and the separation efficiency of the cyclone separator. The separation of grains and short stalks under the action of airflow using the CFD-DEM coupling method has been simulated by Jiang et al. [9], which solved the problem of the indoor settlement of imperfect grains reasonably. The flow characteristics of straw-like slender particles in the flow field has been researched by Cai et al. [10], and a two-way coupling relationship between the slender particles and the flow field has been constructed. Since there are many crops with highly irregular geometric characteristics in the agricultural field, it is urgent to explore an appropriate method to cope with the flow characteristics of such supernormal particles.

There are plenty of calculation methods for particle flow, such as the finite element method based on Lagrange (Euler), the lattice-Boltzmann method and the immersed boundary method [11–13]. The finite element method based on Lagrange (Euler) involves thinking of particles as point sources and then using the Lagrangian method to calculate particle motion, solve fluid interaction with N-S equation, and employ phase interaction to describe the law of particle force and the interaction between particles and walls [14,15]. The lattice-Boltzmann method uses the Boltzmann equation of microscopic statistical mechanics to calculate, and it provides a simplified dynamic model for the microscopic particles in the system. The macroscopic physical quantities of particles (such as density, velocity, etc.) are obtained through mathematical statistical methods, which meet the macroscopic fluid dynamics equations, so this method boasts relatively prominent advantages in describing fluid effects [16,17]. The embedded boundary method proposed by Fadlun et al. uses linear velocity interpolation on the interface between the wall and the fluid to obtain the velocity of the calculated point on the interface and to calculate the interaction force between the fluid and the embedded boundary of the solid wall [18].

Research has shown that a new DEM numerical solution method based on the meshless Galerkin method is being studied by scholars [19–21]. The method uses the weight function and the kernel function to solve the mechanical properties of any point in the region to solve the particle motion problem eventually [22–24]. Instead of mesh generation, it only needs the node information. In addition, it has the advantages of high accuracy, fast convergence, and convenient post-processing. Finally, the meshless Galerkin method eliminates the influence of geometry on the flow to the largest extent; emphasizes the interaction between different particles, between particles and walls, and between particles and fluids; and provides a theoretical basis and mathematical method for solving supernormal particle flow problems.

In summary, the movement of supernormal particle flow is a widespread phenomenon in the agricultural multiphase flow field. However, the understanding of supernormal particle flow in related studies is neither systematic nor in depth, such as that of the mechanical picking of jujube branches, hairy vetch, and straw. The meshless Galerkin method was first used to simulate the motion of supernormal particles, whose numerical results could further reveal the influence of the main flow factors (particle size, particle number and particle force) on the jujube branch. Based on numerical analysis and experimental results, the relationship between sizes of jujube branches, the total feeding number, the rotation speed and shape of the gears and the picking rate of jujube branches were clarified. This research provides a necessary theoretical basis for solving the problem of supernormal particle flow in agricultural machinery engineering, which boasts extensive use prospects and important academic value in the mechanical picking of crop residues.

2. Materials and Methods

2.1. Jujube Branches Model

The jujube branch samples were taken from the jujube garden of the 11th regiment of Alar city, the first division of Tarim, Xinjiang. The cultivation mode was dwarfing culture and compact planting, and the tree was 1 year old, as shown in Figure 1a. The projection method was used to obtain three-dimensional coordinates of critical nodes of the jujube branch, and then the curvature and length of each jujube branch were measured. After modeling, the jujube branch model was produced, as shown in Figure 1b.

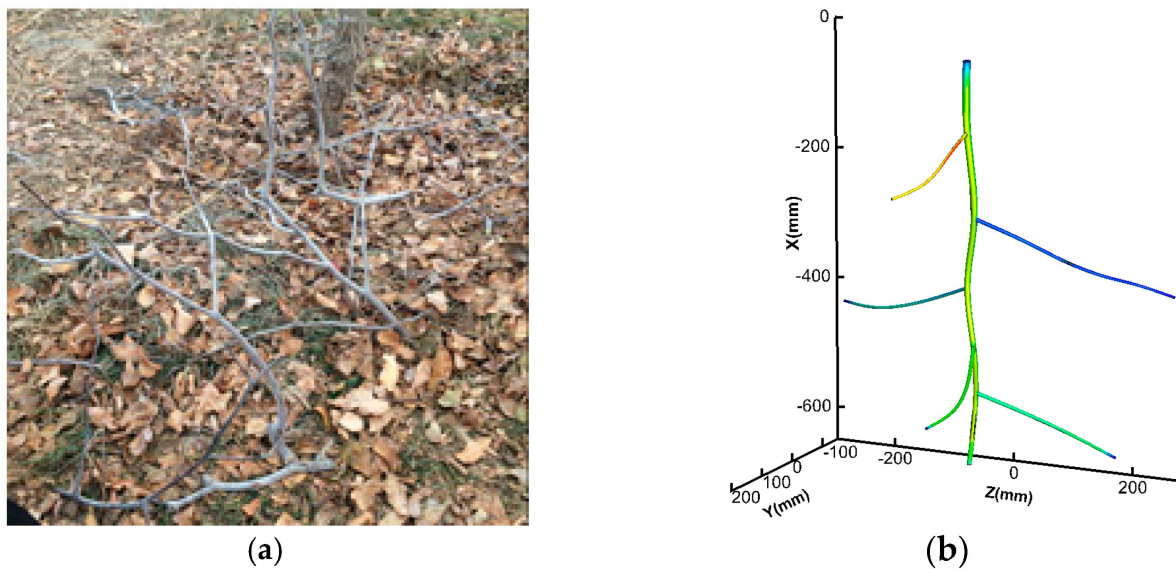


Figure 1. Jujube branch model. (a) Physical map of jujube branches to be picked. (b) Single jujube branch numerical model.

To study the effect of particle size on flow, the selected jujube branches were statistically analyzed to determine the value range of jujube branch size. Test design factors were defined based on the X-direction size of the jujube branch, and the three-level design value of the experiment was determined at the same time. Combined with the randomness principle of the orthogonal experiment, three jujube branch sizes were defined as size I, size II, and size III. The specific jujube branch sizes are shown in Table 1. This physical model does not have the characteristics of spherical particles and can be regarded as a complex supernormal particle.

Table 1. Sizes and parameters of jujube branch.

Jujube Branch Size	Size in X Dimension (mm)	Size in Y Dimension (mm)	Size in Z Dimension (mm)	Surface Area (m ²)	Volume (10 ⁻⁵ m ³)	Weight (kg)	Maximum Screening Size (mm)
Size I	640	370	550	0.038	6.79	0.095	459
Size II	800	463	688	0.059	13.26	0.185	573
Size III	480	278	412	0.021	2.86	0.040	344

2.2. Jujube Picking Mechanism

Figure 2 shows a three-dimensional model of the jujube picking equipment. The equipment is mainly composed of five parts: plane and convey mechanisms, a pair of roller picking mechanisms, crush mechanisms, screen mechanisms and walk mechanisms. The tractor was used as the traction power to realize the field picking process, with the jujube picking equipment connector to the traction frame. In the process of forward movement, the jujube was gathered in front of the shovelling teeth by the rolling brush, and the shovelling teeth were used to transport the jujube branches to the upper and lower gear components to complete the levelling and transportation of the jujube. The jujube could be collected under the action of upper and lower gears. The collected jujube was crushed by the crushing hammer of the crushing device, and the crushing process of the jujube was realized. Through the sieve plates, the crushed straw residue was evenly sprinkled back onto the field. The research emphasis of the equipment is to improve the picking rate, which can not only improve the clogging problem of the collecting system, but also reduce the power consumption; therefore, the research on picking rate is of great significance to the equipment used for picking up branches.

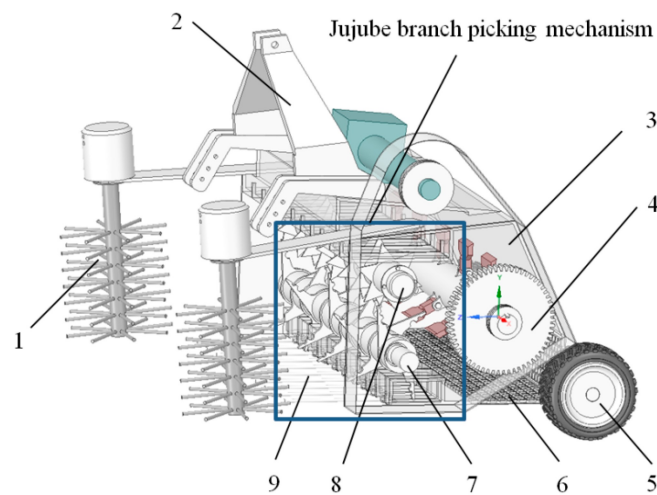


Figure 2. Three-dimensional model of the jujube picking equipment. 1. Rolling brush 2. Traction frame 3. Device shell 4. Crushing mechanism 5. Walking wheels 6. Sieve plates 7. Lower gear assembly 8. Upper gear assembly 9. Collect shovelling teeth.

To obtain the reliable data of the picking rate of the equipment, the numerical simulation model was simplified according to the structure of the test bench, as shown in Figure 3. The rotation direction of the lower gear shaft was opposite to the forward direction, so that the picking mechanism produced a sufficient picking process, the lifting distance and time of the material were extended, and finally, the jujube branches were fully separated. Jujube picking can be regarded as a kind of supernormal particle movement, in which the study of jujube branch size can be regarded as the study of particle size, and the study of total feeding amount can be regarded as the study of the effects of particle number on supernormal particle flow. What is more, the gear will collide with the jujube branch during the rotation, which will affect the speed and direction of the jujube branch. Therefore, the research on the speed of the gear can be regarded as the study of the influence of external force on supernormal particle flow. Due to the frequent occurrence of missing branches during the picking process, the picking rate is an important indicator of jujube picking. The picking rate of jujube branches is shown in Formula (1).

$$Q_1 = \frac{C_1}{S_1} \times 100\% \quad (1)$$

where Q_1 is picking rate, C_1 is the number of jujube branches successfully picked up into the collection box by the jujube picking agency, and S_1 is the total number of jujube branches fed in the picking test.

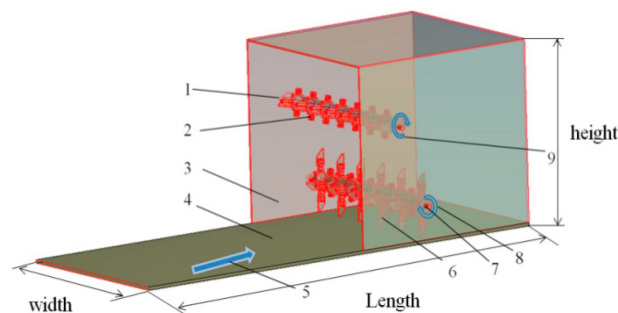


Figure 3. Simplified numerical model of jujube branch picking mechanism. 1. Upper gear shaft 2. Upper gear 3. Device shell 4. Conveyor 5. Movement direction of conveyor belt 6. Lower gear 7. Lower gear shaft 8. Counterclockwise rotation 9. Clockwise rotation.

2.3. Numerical Methods

For the first time, the jujube branch is used as a supernormal particle model, and the meshless Galerkin method was first used to simulate the motion of supernormal particles. This method is to eliminate the influence of the shape of the jujube branch on the flow. Compared with the traditional CFD method, the meshless Galerkin method takes the advantage of not considering the force on the interface between the particles and the flow field, and the effect of particle movement on the mesh deformation of the fluid [25–29]. The study found that the meshless Galerkin method mainly constructs an approximate weight function for the field function according to the node, which is a basic feature of the method. The meshless method includes two key steps: (1) constructing an approximate weight function for the field function; and (2) solving the meshless discretization of partial differential equations.

The jujube branches were transported, entangled, collided, escaped and collected during the mechanical picking process. Among them, the particle size determines the particle weight, the particle force, particle movement speed, and displacement value in the field function. The number of particles affects the relative position between particles, which in turn affects the force between particles and particle movement speed. The gear rotation speed directly affects the force between particles and walls, resulting in changes in particle movement speed and particle displacement. Therefore, the field functions to be calculated are the force, the velocity and the displacement values; the force of the particles is the volume force and the surface force, including the collision force between the particles, the collision contact force, and the rolling force of the particles. The particle movement speed and displacement values were calculated using the current particle position, while speed and time data were used to calculate the relevant data of the particle in the next time step. The specific field function equations are shown in Formulas (2)–(4).

$$m_i \frac{dv_i}{dt} = \sum F_{net} = \sum F_{body} + \sum F_{surface} = \sum F_{body} + \sum F_{contact} + \sum F_{rolling} \quad (2)$$

$$v_{new} = v_{old} + \int_t^{t+\Delta t} \frac{\sum F_{net}}{m} dt \quad (3)$$

$$x_{new} = x_{old} + \int_t^{t+\Delta t} v_{new} dt \quad (4)$$

where m_i is the particle mass at the node x_i , $\text{kg}\cdot\text{m}^{-3}$, F is the particle force, N , v_i is the particle velocity at the node x_i , $\text{m}\cdot\text{s}^{-1}$, x is the particle displacement at the node x_i , m .

The general expression of the equivalent integral form of the differential equation system based on the meshless Galerkin method to solve each node in the domain was calculated using Formula (5).

$$\int_{\Omega_j} wA \left[\sum_{i=1}^n N_i(x)u_i \right] d\Omega_j + \int_{\Gamma_j} \bar{w}B \left[\sum_{i=1}^n N_i(x)u_i \right] d\Gamma_j = 0 \quad (5)$$

where Ω represents the solution domain of the problem, Γ represents the boundary of the solution domain (including displacement boundary and force boundary), A and B are the differential operators of independent variables (such as spatial coordinates, time coordinates, etc.). Functions w and \bar{w} are test functions (or weight functions); $N_i(x)$ is the shape function of the approximate function $u(x)$; u_i is the value of the field function $u(x)$ to be solved at node x_i .

The approximate function $u(x)$ is constructed by solving a set of discrete points $x_i = (i = 1, 2, \dots, N)$ in the domain by solving a set of discrete u_i known in the function $u(x)$, and the expression of the global approximation function $u^h(x)$ at the solution point x_i is:

$$u^h(x, \bar{x}) = \sum_{i=1}^m p_i(\bar{x})a_i(x) = p^T(\bar{x})a(x) \tag{6}$$

where \bar{x} is the coordinate of each node in the solution domain app, $p_i(\bar{x})$ is the basis function, m is the number of basis function, and $a_i(x)$ is the undetermined coefficient.

The primary and secondary basis functions in a two-dimensional space can be expressed as:

$$p^T(\bar{x}) = [1, x, y], m = 3 \tag{7}$$

$$p^T(\bar{x}) = [1, x, y, x^2, xy, y^2], m = 6 \tag{8}$$

The sum of the global approximation function $u^h(x)$ and weight squared error at the solution point is x_i is:

$$J = \sum_j^N w_j \left[\sum_{i=1}^m p_i(\bar{x})a_i(x) - u(x_i) \right]^2 \tag{9}$$

Using the principle of least squares method to solve the undetermined coefficient $a_i(x)$ when $J = 0$, we can obtain:

$$\sum_j^m \left[\sum_{i=1}^N w_i p_i(x_i) p_j(x_j) \right] a_i(x) = \left[\sum_{i=1}^N w_i p_i(x_i) \right] u(x_i) \tag{10}$$

The undetermined coefficient $a_i(x)$ can be obtained from the above formula

$$a(x) = A^{-1}Bu \tag{11}$$

It can be obtained by integrating Equations (6) and (11)

$$u^h(x, \bar{x}) = p^T(\bar{x})A^{-1}Bu = N(x, \bar{x})u \tag{12}$$

The shape function can be obtained as follows:

$$N(x, \bar{x}) = p^T(\bar{x})A^{-1}B \tag{13}$$

The weight function type obtained by the Rocky software is the Gaussian exponential weight function, and its expression is:

$$w_i = \begin{cases} \frac{e^{-(d_i/c_i)^{2k}} - e^{-(r_i/c_i)^{2k}}}{1 - e^{-(r_i/c_i)^{2k}}} & , 0 \leq d_i \leq r_i \\ 0 & , d_i \leq r_i \end{cases} \tag{14}$$

where d_i is the distance from the node x_i to the field point x , m , c_i is the constant of the control function shape, and r_i is the solution domain of the weight function w_i , which is the radius of the node x_i , m .

Under the simulation control of the above equations, jujube branches' movement phenomena, such as transportation, entanglement, collision, escape and collection, occur. Particle size determines the particle mass, which in turn affects particle force, particle movement speed, and the displacement value in the field function. The number of particles affects the position between particles, as well as the force between particles and the speed of particle movement. The rotation speed of the gear directly affects the force between the particles and wall surface, and then affects the particle movement speed and particle displacement.

2.4. Simulation Parameters

Solidworks software was used to draw jujube branch particles and the simplified model of the jujube branch picking mechanism. A full-scale three-dimensional model was imported into the Rocky software, of which the computational domain size was 1.8 m (length) \times 1.3 m (width) \times 1.1 m (height). Firstly, the left side of the model was defined as the entrance of the jujube branch, the translation speed of conveyor belt was set to 0.42 m/s, and the rotation speed and direction of upper and lower gears were given. Secondly, according to the physical parameters of jujube particles, gears, and conveyor belt, the interaction force between particles and gear mechanism, as well as between particles and conveying device, were set. Then, the jujube particle model was input, and the total number of imported particles was determined. Finally, the total calculation time and time step were defined as 20 s and 0.05 s, respectively. Table 2 shows the initial boundary conditions and mechanical parameters of the picking mechanism and jujube branch particles required for the simulation. The design parameters of the prototype machine were taken as reference, and the simulation and experimental data of Ning Xinjie and Almeida E et al. were used to define the physical parameters of jujube branches.

Table 2. Material parameters used in simulation.

Parameters	Values
Translation speed of conveyor belt (m/s)	0.42
Rotating speed of upper and lower gears (r/min)	100, 120 or 150
Total number of particles	16, 23 or 30
Particle shape	I, II or III
Grain density of jujube branch ($\text{kg}\cdot\text{m}^{-3}$)	837
Poisson's ratio of particles	0.5
Shear modulus of particles (Pa)	1.0×10^9
Coefficient of restitution between particles	0.5
Coefficient of static friction between particles	0.45
Coefficient of dynamic friction between particles	0.08
Density of the gear mechanism (steel, $\text{kg}\cdot\text{m}^{-3}$)	7800
Poisson's ratio of gear mechanism	0.3
Shear modulus of gear mechanism (Pa)	7×10^{10}
Coefficient of static friction between particles and gear shifting mechanism	0.35
Coefficient of dynamic friction between particles and gear shifting mechanism	0.04
Restitution coefficient of particles and gear shifting mechanism	0.5
Conveying device (rubber, $\text{kg}\cdot\text{m}^{-3}$)	1400
Poisson's ratio of conveying device	0.3
Shear modulus of conveying device (Pa)	1×10^{11}
Coefficient of static friction between particles and conveying device	0.9
Coefficient of dynamic friction between particles and conveying device	0.1
Restitution coefficient of particles and conveying device	0.5
Calculation of total time (s)	20
Time step (s)	0.05

3. Results and Discussions

3.1. Numerical Analysis of Movement during Jujube Branch Picking

Figure 4 shows the dynamic analysis results obtained by the Rocky software. The simulation time is 20 s; the filling time of jujube branches varied from 0 s to 16 s with an average speed of one jujube branch per second. Jujube branches were conveyed, entangled, collided, escaped, and collected on the conveying device and picking mechanism. Figure 4a shows the state of jujube branches after the filling time of 4 s. Meanwhile, four jujube branches were piled up on the conveyor belt, and the first jujube branch was rolled sideways by the action of the gear shift. Figure 4b shows the state of jujube branches at 10 s, when the counter-roller gear starts to pick up the first jujube branch. Then, under the influence of gear and adjacent jujube branches, jujube branches close to the gear tooth begin to

collide and roll, which results in the escape of jujube branches. Figure 4c shows that jujube branches within the dotted line were leaving the test bed under the impact of collision when the time was 13.9 s. Under the working condition of this analysis, a total of three jujube branches fell off from the test bed, all of which slipped from the edge of the conveyor belt after collision and winding. Figure 4d shows that one jujube branch was successfully collected at 16.9 s. When jujube branches were regarded as supernormal particles, the meshless Galerkin method (MGM) could be used to describe the dynamic process of jujube branch movements, such as transportation, collision, and tumbling.

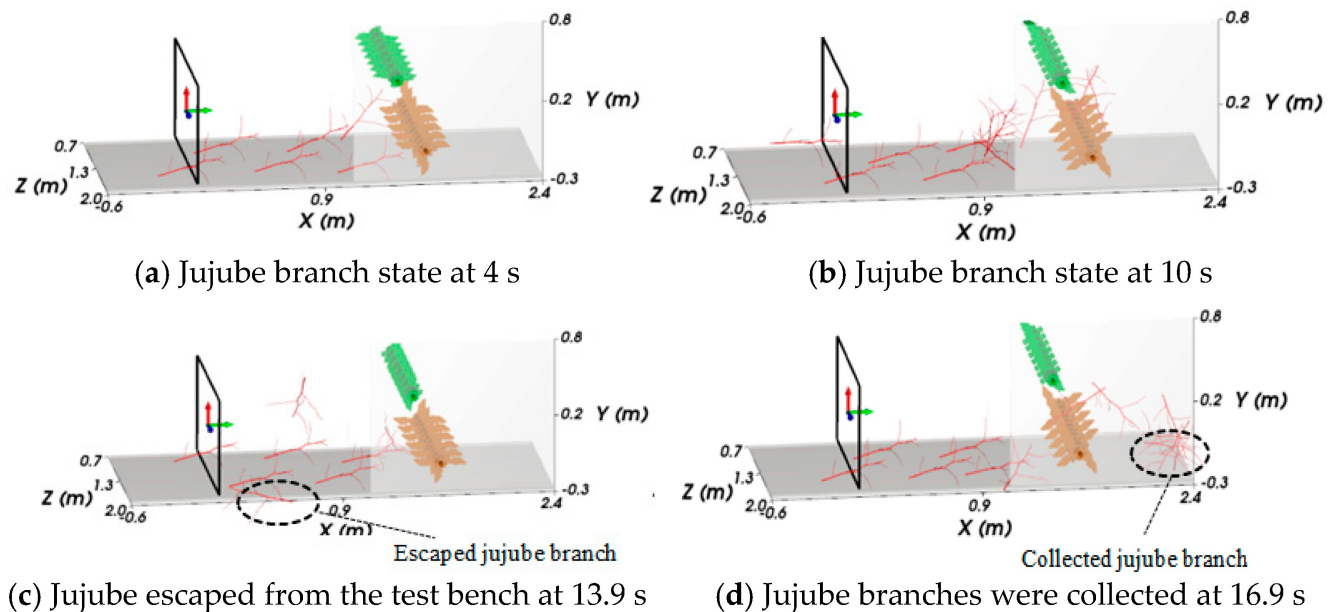


Figure 4. Dynamic picking process of jujube branches.

3.2. Influence of Jujube Branch Size on Picking Rate

In order to study the relationship between the size and picking rate of jujube branches, a numerical analysis was carried out on the movement law and picking rate changes for three sizes of jujube branches in the picking progress.

Figure 5a shows the movement of the simulation at the time point of 10.65 s when a total of 16 jujube branches with a size of 480 mm were fed. It can be found that the feeding was more uniform because the number of jujube branches was relatively small and there was little interference among each other. At the same time, due to the smaller size of the jujube branch, the weight was correspondingly lighter. Further study of the dynamic process showed that only winding and rolling occurred after the collision of jujube branches, not flinging. It is concluded that when the jujube branch was lighter, the force caused by collision can be reduced, the distance that the jujube branch was pushed away by the gear was shorter, and there was less rolling, which is beneficial to the final collection. Figure 5b shows the jujube branch's movement when jujube branch size was 640 mm and fed with a total of 23 jujube branches. As shown in the figure, due to the increase in the size of the jujube branches, the force between the jujube branch and the shifting teeth was more potent, resulting in throwing off the jujube branch. In addition, the jujube branch and the shifting teeth were also entangled due to the increase in twig size, leading to the decrease in the picking rate. Figure 5c shows the movement of jujube branches when the size of jujube branch was 800 mm and the total amount of jujube branch feeding was 30. As the size of jujube branches increased, the mass of a single particle also increased, but the amount of the dialing power of the dial tooth was limited; it was difficult for the dial tooth to dial the jujube branch, causing the jujube branches to pile up on each other. However, the jujube branches were transported by the conveyor belt and entered between the two gears, and then they were finally collected after throwing out the equipment under the agitation of

the gears. The simulation results showed that large-size jujube branches were helpful for collection due to the influence of weight and size. The impact of the collision caused by the shifting of the teeth only causes the jujube branch to roll, and the rolling jujube branch will have an entanglement and rolling influence on the subsequent jujube branch.

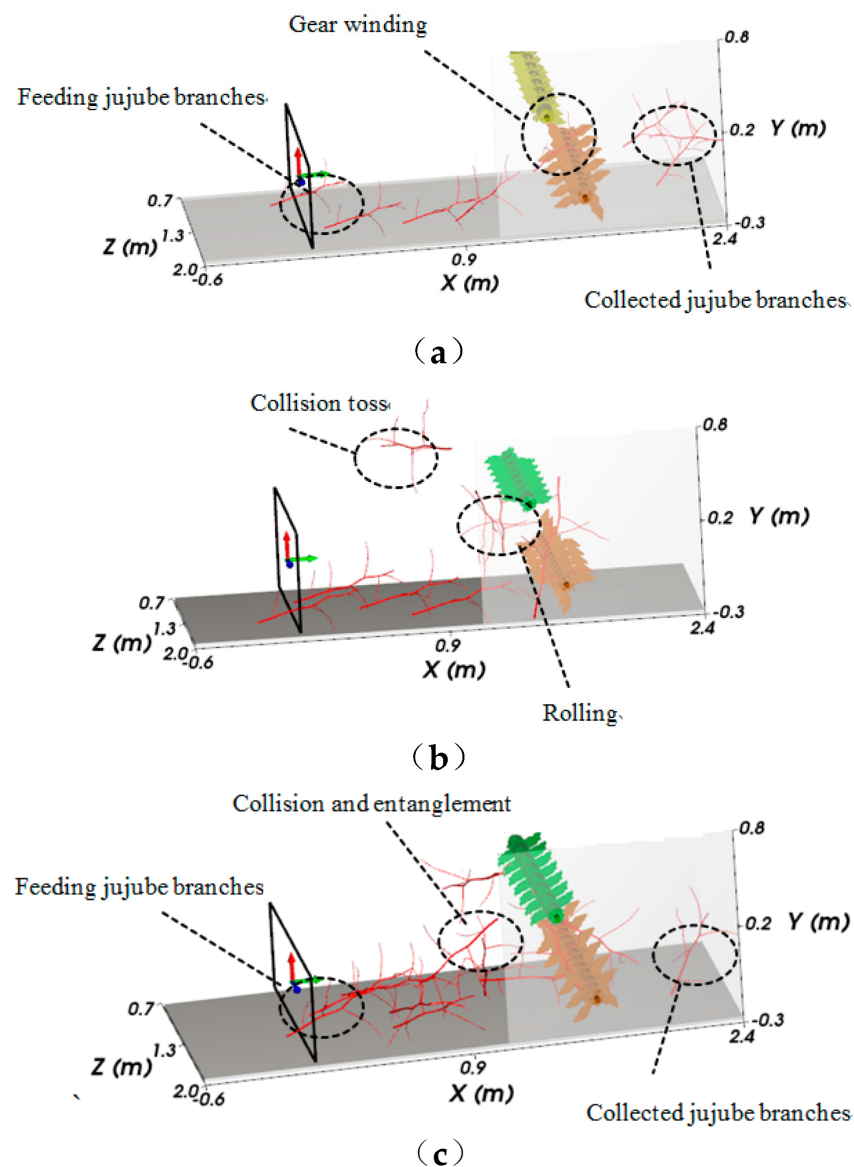


Figure 5. Movement behavior analysis of jujube branches in the picking mechanism. (a) State of jujube branches with a size of 480 mm when the time point is 10.65 s. (b) State of jujube branches with a size of 640 mm when the time point is 12.9 s. (c) Collection state of jujube branches with a size of 800 mm when the time point is 13.65 s.

In this research, the influence of the size of jujube branches on the picking up rate of jujube branches was obtained by single-factor analysis with experimental and numerical results (Figure 6). It can be found from Figure 6 that the picking rate of the test result was higher than that of the numerical simulation, the curve of the test result has relatively smaller fluctuation, and the numerical result has a deviation between the two values at the size of 640 mm. Further research on the number of jujube branches found that when the size is 640 mm, the number of jujube branches collected in the numerical result is 13 and the test result is 15, with the deviation between the two being 2.

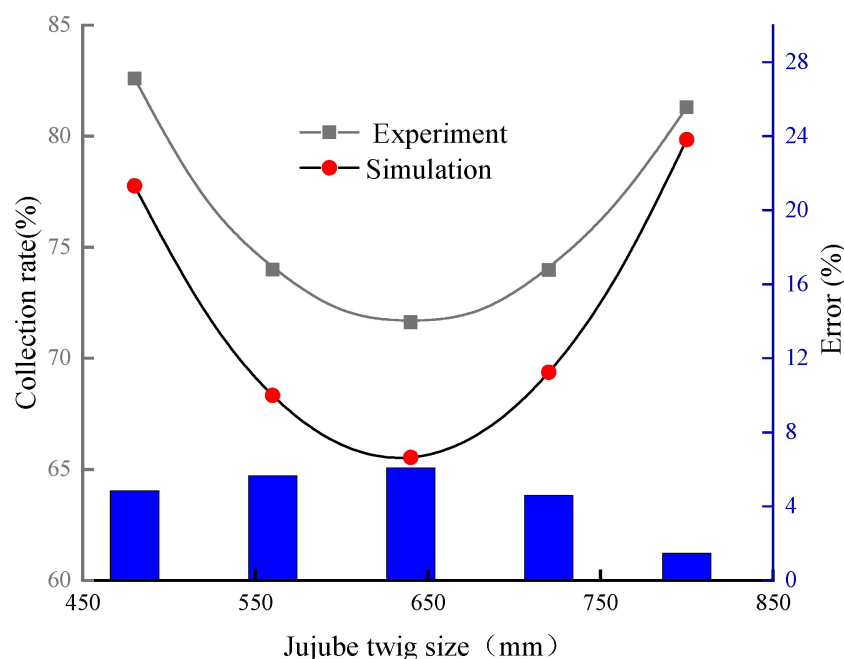


Figure 6. Relationship between jujube branch size and picking rate.

The experimental and numerical results show that the influence of jujube branch size on the picking is parabolic distribution. When the size of jujube branches is 480 mm and 800 mm, the picking rate of jujube branches can reach 75%. Combined with the analysis of the field function equation, it can be found that the particle size of the jujube branch is one of the important factors affecting the particle movement. According to the field function equation, the particle size determines the mass m_i of a single particle and affects the volume force F_{body} of the particle. In addition, the particle size also influences the contact force F_{contact} and tumbling force F_{rolling} . At the same time, according to the weight function equation, it can be found that the particle size is related to the distance d_i from the node x_i of the weight function to the field point x and the radius r_i of the support domain. The change in the particle size will inevitably affect the value of the weight function.

3.3. Influence of the Total Number of Jujube Branches on Picking Rate

When the feeding number was 16, 23, or 30, the influence of the total feeding number on the picking rate was analyzed. Figure 7 shows the relationship between the numbers of jujube branches collected at the exit of the picking mechanism over time. The figure shows that the jujube branch collection process was irregular because the collision among jujube branches and between jujube branches and the wall affect the movement of the jujube branches. In the process of $t = (0, 10 \text{ s})$, the number of jujube branches collected was smaller, and with time, the number of jujube branches increases. Figure 7a shows the process of $t = (14 \text{ s}, 20 \text{ s})$: the collection number and time were relatively uniform, indicating that the collection effect was better. The numerical calculation result of the picking rate under this working condition was 75%. Figure 7b shows that during the $t = (13 \text{ s}, 20 \text{ s})$ process, the distribution of the number of collections was not uniform, as shown in Figure 7a, indicating that the jujube branches interfere with each other during the collection process. The numerical calculation result of the picking rate under this working condition was 56.6%. In Figure 7c, the feeding number of jujube branches was the most, and the interaction among jujube branches was the most intense. When $t = 9 \text{ s}$, this influence begins to take effect in the collection process.

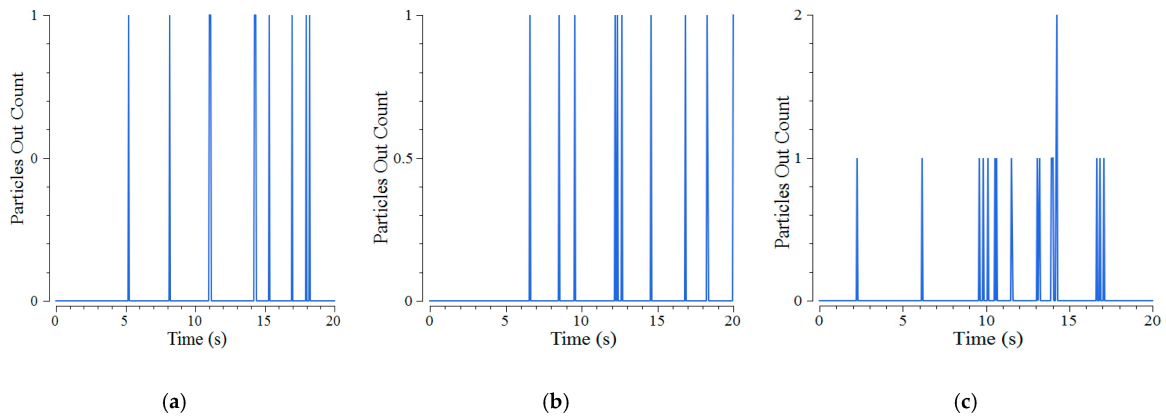


Figure 7. Relationship between the numbers of jujube branches collected over time. (a) Feed 16 jujube branches. (b) Feed 23 jujube branches. (c) Feed 30 jujube branches.

Figure 8 shows the effect of the total feeding number on the movement of jujube branches. From Figure 8a, it can be found that the three adjacent jujube branches at the entrance were relatively far apart, which reduces the entanglement and collision of the jujube branches in the tooth setting area. With the increase in the number of particles, the distance among the three adjacent jujube branches at the entrance became smaller, and the collision and entanglement of the jujube branches in the area of the teeth increased, as shown in Figure 8b. When the number of jujube branches increased to 30, the jujube branches overlapped and were arranged in a staggered manner (Figure 8c), and collision and entanglement may occur during the movement.

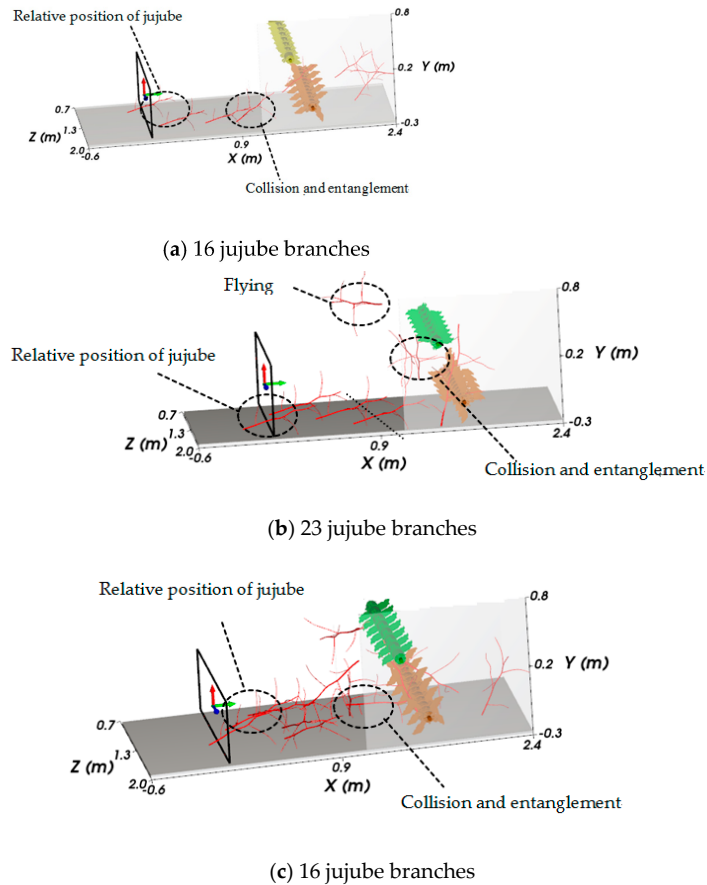


Figure 8. Effect of the total number of jujube branches fed on the movement position of jujube branches.

As the total feeding number increases, both the value and the test results show a trend of first declining and then rising, as shown in Figure 9. The increase in jujube branches leads to more serious interference between jujube branches, and the probability of entanglement collision and jujube branch escape increases. When the number reaches a certain level, the entanglement and collision of jujube branches will increase the picking rate of jujube branches.

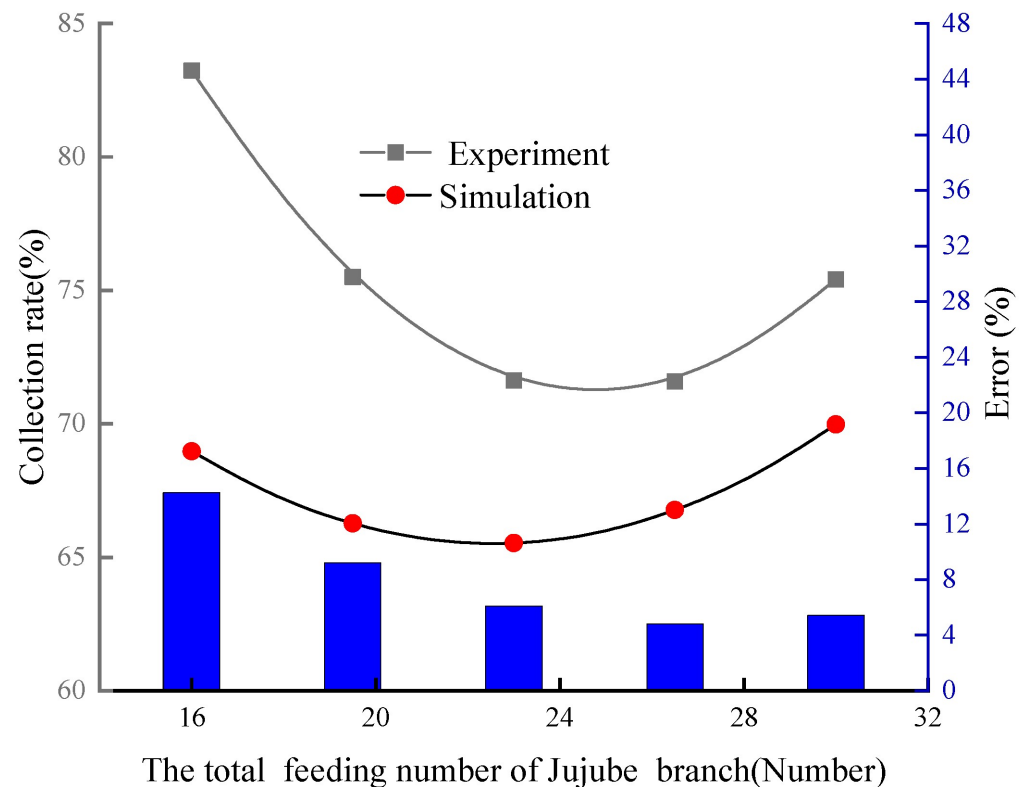


Figure 9. Relationship between the total number of jujube branches and the picking rate.

The total feeding number of jujube branches does not affect the quality and geometric properties of a single particle, nor does it affect the distance d_i from the weight function node x_i to the field point x and the support domain radius r_i . According to the field function equation, the total number of feeds affects the contact force F_{contact} between particles, and influences the collisions between different particles, as well as between particles and walls. Compared to the size of jujube branches, the total feeding number affects the picking rate of jujube branches less.

3.4. Influence of Gear Rotation Speed on Picking Rate

The jujube branch picking mechanism makes collisions among jujube branches as well as collisions between jujube branches and the wall surface through the dialing of the teeth, which form a granular force. At the same time, with the appearance of tumbling, collision, entanglement, and throwing, the picking rate changes. When the gear rotation speed was 100 r/min, the collision and force between the jujube branch and the gear may be small, and the entanglement and throwing phenomenon may be rarer (Figure 10a). When the gear rotation speed increases to 120 r/min, the force of the gear on the jujube branch increases, and collisions and throws become more frequent (Figure 10b). When the rotation speed reaches 150 r/min, the force of the shifting tooth is further strengthened, and the number of jujube branches that are shifted away increases (Figure 10c).

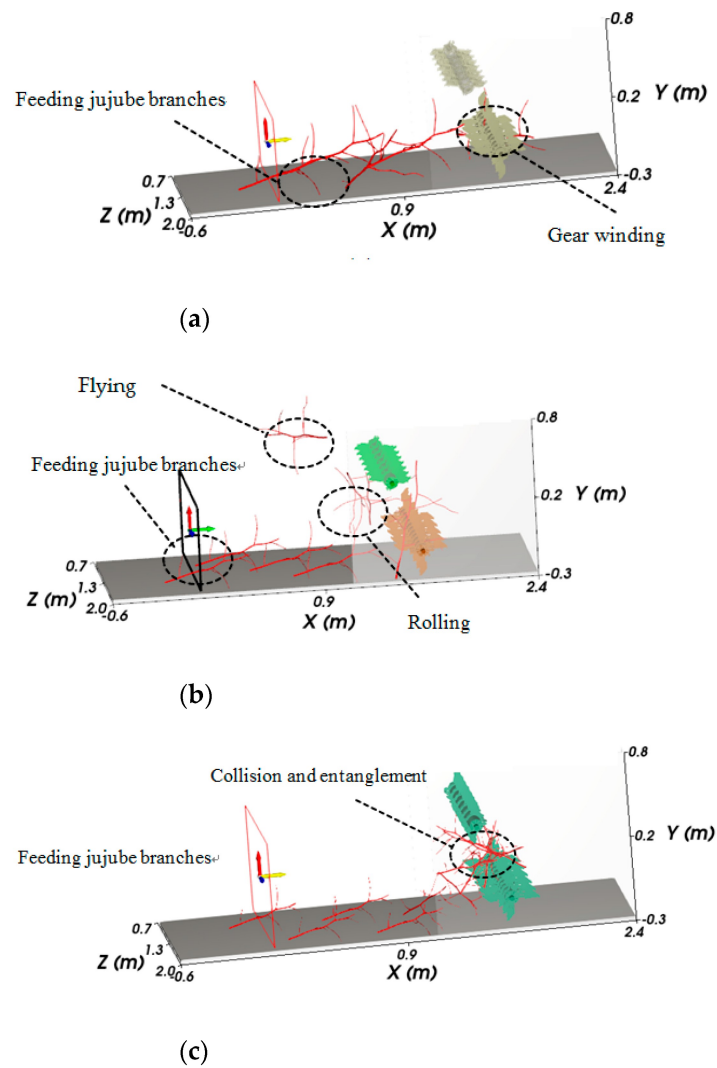


Figure 10. Influence of the gear rotation speed on the movement of jujube branches. (a) Gear rotation speed is 100 r/min. (b) Gear rotation speed is 120 r/min. (c) Gear rotation speed is 150 r/min.

It can be found from Figure 11 that with the increase in gear rotation speed, the collision effect between particles becomes stronger and the particle pickup rate decreases.

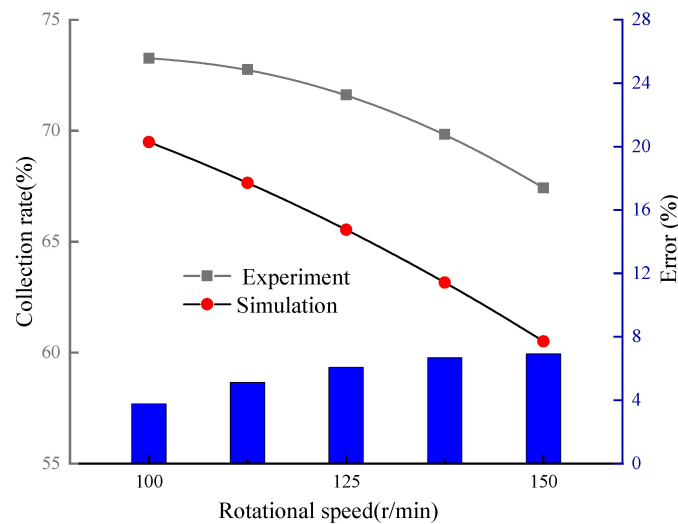


Figure 11. Relationship between gear speed and picking rate.

Numerical simulation values and test results show that the increase in the rotation speed of the gear makes the interaction between the particles more serious and reduces the picking rate of jujube branches. Compared with the size of the jujube branch and the total number of feeds, the speed of the gear shift affects the particle contact force and tumbling force less than the size of the jujube branch and more than the total number of feeds.

3.5. Orthogonal Test Verification

Figure 12 shows an experimental prototype of the jujube picking mechanism, which is mainly composed of a pair of roller picking mechanisms, an electromagnetic speed regulating motor, a conveyor belt mechanism, a chain drive system, a collection box, and a JD1 electromagnetic speed regulating motor inverter. The jujube branch samples were placed on the conveying device, which moved steadily under the drive of the frequency conversion motor. The jujube branch samples were transported to the picking area of the pair-roller picking mechanism, and the picking mechanism performed a pair-roller picking movement to pick up the jujube branch samples on the conveyor belt and move them to the collection box.

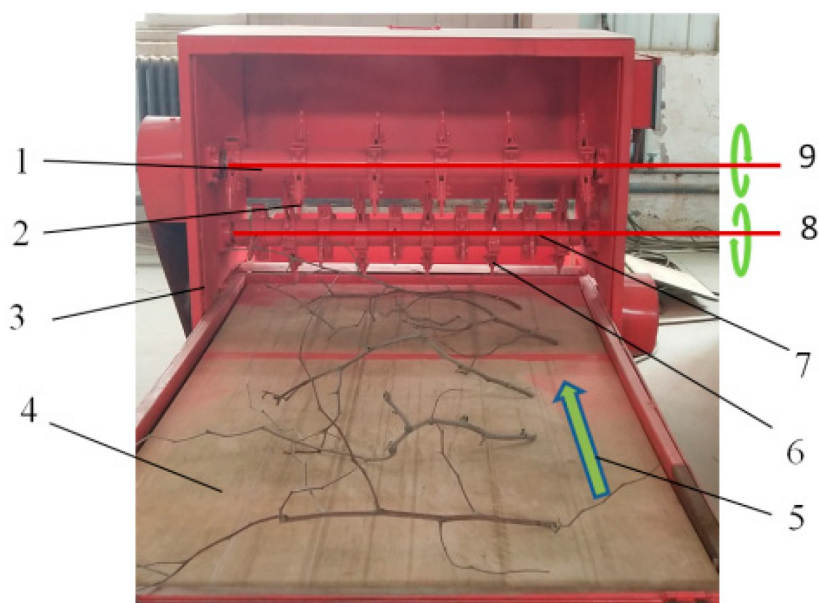


Figure 12. Prototype of jujube branch picking mechanism. 1. Upper gear shaft 2. Upper gear 3. Device shell 4. Conveyor 5. Movement direction of conveyor belt 6. Lower gear 7. Lower gear shaft 8. Counterclockwise rotation 9. Clockwise rotation.

The jujube picking mechanism test device was used for orthogonal test verification. Each variable parameter was set, among which the size of the jujube branches was 480 mm, 640 mm and 800 mm; the total number of feedings was 16, 23 and 30; and the rotation speed of the gear was 100 r/min, 120 r/min, and 150 r/min. The test plan L9 (3⁴) was selected, and the orthogonal test was performed according to the randomness principle of the orthogonal test, as shown in Table 3.

Table 3. Influence factors and levels of test.

Factors	A	B	C
Level	Total Number of Feeding (Branch)	Size of Jujube Branch (mm)	Rotation Speed of the Gear (r/min)
1	16	640	150
2	23	800	100
3	30	480	120

As shown in Table 4, numerical simulation values and test results showed that the size of jujube branches was an important factor affecting the picking rate. The picking rate of jujube branches was the worst when the size of jujube branches was 640 mm. When the size of jujube branches was 800 mm and 480 mm, the picking rate of jujube branches was relatively higher. From the numerical value and the test results, the picking rate was highest when the jujube branch size was 480 mm, which indicated that the jujube branches with a smaller size were easier to be collected.

Table 4. Experimental design and comparative analysis with simulation results.

Test Number	Factors				Test Results	Numerical Results
	A Total Number of Feeding (branch)	B Size of Jujube Branch (mm)	Test Error	C Rotation Speed of the Gear (r/min)	Picking Rate (%)	
1	1	1	1	1	75	62.5
2	1	2	2	2	81.3	75
3	1	3	3	3	81.3	75
4	2	1	2	3	65.2	56.6
5	2	2	3	1	82.6	73.9
6	2	3	1	2	82.6	73.9
7	3	1	3	2	60	56.7
8	3	2	1	3	76.7	70
9	3	3	2	1	86.7	73.3
Test analysis	k1	237.6	200.2	234.3	244.3	
	k3	230.4	240.6	233.2	223.9	
	k2	223.4	250.6	223.9	223.2	
	R	14.2	50.4	10.4	21.1	
	Optimal order of factors			B > C > A B ₃ C ₁ A ₁		
Numerical analysis	k1	212.5	175.8	206.4	209.7	
	k3	204.4	218.9	204.9	205.6	
	k2	200	222.2	205.6	201.6	
	R	12.5	46.4	1.5	8.1	
	Optimal order of factors			B > A > C B ₃ C ₁ A ₁		

The extreme difference between the gear rotation speed and the total number of jujube branch feeds was relatively close, and the effect on the picking rate was basically the same. From the perspective of the optimal plan, the test results were consistent with the numerical results. The optimal plan was B₃C₁A₁, which means that when the jujube branch size was 480 mm, the total number of jujube branches was 16 and the gear rotation speed was 150 r/min, the picking rate was the highest. The test results proved the reliability of the numerical results, indicating that the use of numerical methods based on the meshless Galerkin method can solve the problem related to supernormal particle flow in the process of picking up jujube branches.

4. Discussion

The numerical analysis method provides an important research method for the research and development of the pick-up equipment of jujube branches. The method can effectively simulate the pick-up process of jujube branches and obtain the important factors. It is not difficult to find out that the core of the influence on the picking rate is the collision and winding of jujube branches. In addition to the above factors, the shape of the gear is also an important factor. Using the optimal total feeding number, the size of jujube branches and the rotation speed of the gear, the shape of the gear can be further simulated and tested, and its influence on the picking rate can be obtained. Figure 13 shows three gear shapes (the unit of size is mm), where gear 2 is the initial design gear and gear 1 and 3 are the modified shapes.

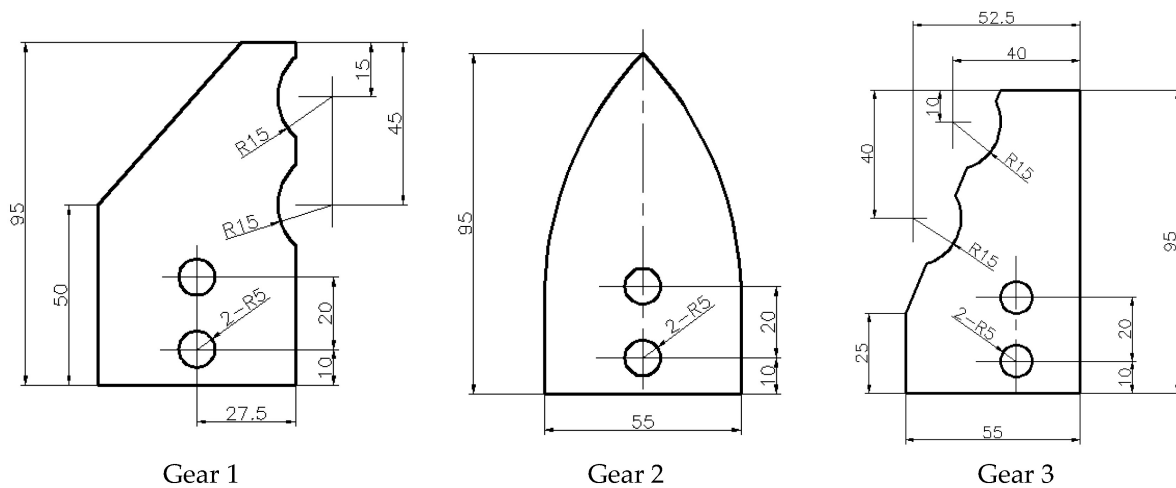


Figure 13. Gear Profile.

The collection situation of the jujube branch picking process could be obtained quickly using the numerical simulation method. Figure 14 shows the gear 3 collection of jujube branches. In the process of 12~20 s, when the interval of collecting jujube branches was relatively stable, the number of collected jujube branches was almost the same, with 21 jujube branches out of the total input of 24 being collected and the collection efficiency being 87.5%.

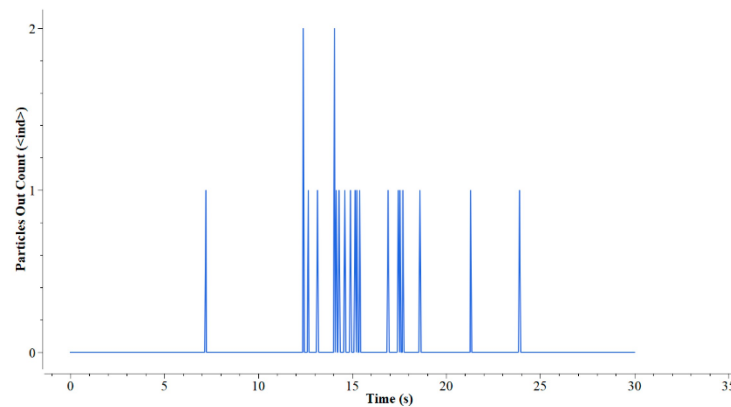


Figure 14. Collection of jujube branches on gear 3.

The relevant experimental research on the gear profile was carried out, and Table 5 shows the parameters involved in the experiment. The experimental results under the influence of a single factor of tooth profile are obtained by repeatedly testing different gears five times and by taking the average value of five data. The experimental data show that the picking rate is 83.3% when gear 3 is used, which is close to the numerical results.

Table 5. Experimental design on single-factor effect test of tooth profile.

Factors	Height of Gear (cm)	Gear Pitch (cm)	Rotation Speed (r/min)	Number of Feeding	Pick Up a Number	Picking Rate
Gear1	13.5	10	150	24	17	70.8%
Gear2	13.5	10	150	24	15	62.5%
Gear3	13.5	10	150	24	20	83.3%

5. Conclusions

The meshless Galerkin method (MGM) is an effective solution for problems related to supernormal and irregular particles. Without gridding the supernormal particles in the computational domain, the dynamic movement process of supernormal particles such as transportation, collision, throwing, and tumbling can be described only by constructing approximate weight functions and solving partial differential equations with the field function (particle force, particle movement velocity, and displacement value). In this paper, the meshless Galerkin method (MGM) and the method of combining numerical simulation and experimental verification are employed to study the influence of jujube branch size (particle size), the total number of feeds (number of particles), and the gear rotation speed and shape (particle force) on the picking rate of jujube branches.

- (1) The numerical and experimental results show that the size of jujube branches not only affected the entire field function, but also influenced the weight function, which was an important factor affecting the picking rate of jujube branches. The influence curve of jujube branch size on the picking rate presented a parabolic distribution. When the jujube branch size was 480 mm and 800 mm, the jujube picking rate could reach a peak of 75%.
- (2) The total feeding number and the rotation speed of the gear also have an effect on the picking rate of jujube branches. These two factors will affect the force between the particles, the particles and the wall, and the force of the particles in the field function, causing the jujube branches to roll, collide, entangle, and flutter.
- (3) With the increase in the number of particles, the picking rate presented a parabolic distribution, with the minimum trough values being 65.5 and 71.1% and the maximum peak values being 69.9% and 83.2%, respectively. The rotation speed of the gear is in a negative correlation with the picking rate, which means the smaller the speed is, the higher the collection rate of jujube branches will be, with the value and the maximum picking rate in the experiment being 69.5% and 73.2%, respectively.

Author Contributions: Formal analysis, J.H.; Funding acquisition, W.W.; Investigation, X.Y.; Project administration, W.W.; Software, D.R.; Supervision, W.W.; Validation, Y.G.; Writing—original draft, R.Z. and G.W.; Writing—review and editing, W.W. and M.Y. All authors have read and agreed to the published version of the manuscript.

Funding: This research was funded by National Nature Science Foundation of China, grant number 32171900.

Institutional Review Board Statement: Not applicable.

Data Availability Statement: Not applicable.

Acknowledgments: The authors would like to thank the research team members for their contributions to this work.

Conflicts of Interest: The authors declare no conflict of interest.

References

1. Ma, Z.; Li, Y.; Xu, L.; Chen, J.; Zhao, Z.; Tang, Z. Dispersion and migration of agricultural particles in a variable-amplitude screen box based on the discrete element method. *Comput. Electron. Agric.* **2017**, *142*, 173–180. [[CrossRef](#)]
2. Jebahi, M.; Dau, F.; Charles, J. Multiscale Modeling of Complex Dynamic Problems: An Overview and Recent Developments. *Arch. Comput. Methods Eng.* **2016**, *23*, 101–138. [[CrossRef](#)]
3. Tchen, C. Mean Value and Correlation Problem Connected with the Motion of Small Particles Suspended in a Turbulent Fluid. Ph.D. Dissertation, Delft University, Martinus Nijhoff, Hague, The Netherlands, 1947.
4. Kafashan, J.; Wiącek, J.; Abd Rahman, N.; Gan, J. Two-dimensional particle shapes modelling for DEM simulations in engineering: A review. *Granul. Matter* **2019**, *21*. [[CrossRef](#)]
5. Ito, S.; Nagatani, T.; Saegusa, T. Volatile jam and flow fluctuation in counter flow of slender particles. *Physica A* **2007**, *373*, 672–682.
6. Dosta, M.; Antonyuk, S.; Broeckel, U. DEM simulations of amorphous irregular shaped micrometer-sized titania agglomerates at compression. *Adv. Powder Technol.* **2015**, *26*, 767–777.

7. Fanyi, L. *Discrete Element Modelling of the Wheat Particles and Short Straw in Cleaning Devices*. PhD Thesis; Northwest A and F University: Shanxi, China, 2018.
8. Xin, J.M.; Chen, T.Y.; Meng, J.; Wu, L.Y.; Jiao, J.K.; Zhang, Q.; Liu, C.H.; Song, Y.Q.; Ren, W.T. Design and numerical simulation of two-stage device for dust removal from flue gas of straw carboniz. *J. Huazhong Agric. Univ.* **2018**, *37*, 100–107.
9. Jiang, E.; Sun, Z.; Pan, Z.; Wang, L. Numerical simulation based on CFD-DEM and experiment of grain moving laws in inertia separation chamber. *Trans. Chin. Soc. Agric. Mach.* **2014**, *45*, 117–122.
10. Cai, J.; Zhao, X.B.; Geng, F. Numerical study on the fluidization characteristics of slender particles with gas/solid two-way coupling. *Acta Energ. Sol. Sin.* **2018**, *21*, 3169–3177.
11. Guoxiang, S.; Yongbo, L.; Xiaochan, W.; Yu, J. CFD simulation and experiment of distribution characteristics for droplet of knapsack sprayer. *Trans. Chin. Soc. Agric. Eng.* **2012**, *28*, 73–79.
12. Han, D.; Zhang, D.; Yang, L.; Li, K.; Zhang, T.; Wang, Y.; Cui, T. EDEM-CFD simulation and experiment of working performance of inside-filling air-blowing seed metering device in maize. *Trans. Chin. Soc. Agric. Eng.* **2017**, *33*, 23–31.
13. Du, J.; Hu, G.M.; Fang, Z.Q. Accelerating CFD-DEM simulation of dilute pneumatic conveying with bends. *Int. J. Fluid Mach. Syst.* **2015**, *8*, 84–93. [[CrossRef](#)]
14. Hua, L.; Meina, Z.; Wenqing, Y. Optimization of airflow field on air-and-screen cleaning device based on CFD. *Trans. Chin. Soc. Agric. Mach.* **2013**, *44*, 12–16.
15. Tsuji, Y.; Kawaguchi, T.; Tanaka, T. Discrete particle simulation of two-dimensional fluidized bed. *Powder Technol.* **1993**, *77*, 79–87. [[CrossRef](#)]
16. Han, H.F. Numerical Study on Gas-Solid Two-Phase Flow Based on the Lattice Boltzmann Method: Direct Numerical Simulation and Efficient Implementation. Ph.D. Thesis, Huazhong University of Science and Technology, Wuhan, China, 2013.
17. Chen, L.; Mo, C.; Wang, L.; Cui, H. Direct numerical simulation of the self-propelled Janus particle: Use of grid-refined fluctuating lattice Boltzmann method. *Microfluid. Nanofluidics* **2019**, *23*, 73.1–73.16.
18. Wang, Z.L. Fully Resolved Direct Numerical Simulation Technique and Its Application in Multiphase Flows. Ph.D. Thesis, Zhejiang University, Zhejiang, China, 2010.
19. Thomas, S. Meshless methods: An overview and recent developments. *Comput. Methods Appl. Mech. Eng.* **2005**, *139*, 3–47.
20. Zhang, X. Application of Meshless Local Petrov-Galerkin Method in Large Deformation Problems. Ph.D. Thesis, Tsinghua University, Beijing, China, 2006.
21. Zeng, H.Q. Parallel algorithms and parallel implementation of meshless numerical simulation. Ph.D. Thesis, University of Science and Technology of China, Hefei, China, 2006.
22. Pan, X.F.; Zhang, X.; Lu M, W. Meshless Galerkin least-squares method. *Comput. Mech.* **2005**, *35*, 182–189.
23. Keck, R.; Hietel, D. A projection technique for incompressible flow in the meshless finite volume particle method. *Adv. Comput. Math.* **2005**, *23*, 143–169.
24. Zhang, Q.; Banerjee, U. Numerical integration in Galerkin meshless methods, applied to elliptic Neumann problem with non-constant coefficients. *Adv. Comput. Math.* **2012**, *37*, 453–492. [[CrossRef](#)]
25. Xu, Z.; Chun, F.Z.; Wan, M.Z.; Yang, F. Discrete element simulation and its validation on vibration and deformation of railway ballast. *Yantu Lixue/Rock Soil Mech.* **2017**, *38*, 1481–1488.
26. Xinjie, N.; Chengqian, J.; Xiang, Y. Research status and development trend of air and screen cleaning device for cereal combine harvesters. *J. Chin. Agric. Mechmination* **2018**, *39*, 9–14.
27. Zhang, F.Q. The Application of Smoothed Particle Hydrodynamics Method in Structure Analysis. Master's Thesis, Nanjing University of Aeronautics and Astronautics, Nanjing, China, 2007.
28. de Almeida, E.; Spogis, N.; Taranto, O.P.; Silva, M.A. Theoretical study of pneumatic separation of sugarcane bagasse particles. *Biomass Bioenergy* **2019**, *127*, 105256.
29. Almeida, E. Exploratory Study of Rocky/Fluent Software Coupling-Case: Pneumatic Separation of Sugarcane Bagasse Particles. Ph.D. Thesis, University of Campinas, Campinas, Brazil, 2018.

Disclaimer/Publisher's Note: The statements, opinions and data contained in all publications are solely those of the individual author(s) and contributor(s) and not of MDPI and/or the editor(s). MDPI and/or the editor(s) disclaim responsibility for any injury to people or property resulting from any ideas, methods, instructions or products referred to in the content.